Angiogenic activities are increased via upregulation of HIF-1α expression in gefitinib-resistant non-small cell lung carcinoma cells

JEONG EUN CHA[1*], WOOM-YEE BAE[1,2*], JAE-SUN CHOI[2,3], SEUNG HYEUN LEE[4] and JOO-WON JEONG[1,2]

[1]Department of Biomedical Science, Graduate School; [2]Department of Anatomy and Neurobiology, College of Medicine; [3]Medical Science Research Institute; [4]Division of Pulmonary, Allergy and Critical Care Medicine, Department of Internal Medicine, College of Medicine, Kyung Hee University, Seoul 02447, Republic of Korea

Received March 11, 2021; Accepted June 30, 2021

DOI: 10.3892/ol.2021.12932

Abstract. Epidermal growth factor receptor (EGFR)-tyrosine kinase inhibitors (TKIs) have been used to treat patients with non-small cell lung cancer (NSCLC) and activating EGFR mutations; however, the emergence of secondary mutations in EGFR or the acquisition of resistance to EGFR-TKIs can develop and is involved in clinical failure. Since angiogenesis is associated with tumor progression and the blockade of antitumor drugs, inhibition of angiogenesis could be a rational strategy for developing anticancer drugs combined with EGFR-TKIs to treat patients with NSCLC. The signaling pathway mediated by hypoxia-inducible factor-1 (HIF-1) is essential for tumor angiogenesis. The present study aimed to identify the dependence of gefitinib resistance on HIF-1α activity using angiogenesis assays, western blot analysis, colony formation assay, xenograft tumor mouse model and immunohistochemical analysis of tumor tissues. In the NSCLC cell lines, HIF-1α protein expression levels and hypoxia-induced angiogenic activities were found to be increased. In a xenograft mouse tumor model, tumor tissues derived from gefitinib-resistant PC9 cells showed increased protein expression of HIF-1α and angiogenesis within the tumors. Furthermore, inhibition of HIF-1α suppressed resistance to gefitinib, whereas overexpression of HIF-1α increased resistance to gefitinib. The results from the present study provides evidence that HIF-1α was associated with the acquisition of resistance to gefitinib and suggested that inhibiting HIF-1α alleviated gefitinib resistance in NSCLC cell lines.

Correspondence to: Professor Joo-Won Jeong, Department of Anatomy and Neurobiology, College of Medicine, Kyung Hee University, 26 Kyunghee-daero, Dongdaemun-gu, Seoul 02447, Republic of Korea
E-mail: jjeong@khu.ac.kr

Professor Seung Hyeun Lee, Division of Pulmonary, Allergy and Critical Care Medicine, Department of Internal Medicine, College of Medicine, Kyung Hee University, 26 Kyunghee-daero, Dongdaemun-gu, Seoul 02447, Republic of Korea
E-mail: humanmd04@daum.net

*Contributed equally

Abbreviations: NSCLC, non-small cell lung cancer; EGFR, epidermal growth factor receptor; TKI, tyrosine kinase inhibitor; HIF-1α, hypoxia-inducible factor-1α; GR, gefitinib-resistant

Key words: gefitinib, NSCLC, HIF-1α, angiogenesis, EGFR-TKIs

Introduction

Lung cancer is the most common cause of cancer-associated mortality worldwide (1). The majority (80-85%) of all lung cancers are non-small cell lung cancer (NSCLC) (2), which is characterized by multiple mutations in the epidermal growth factor receptor (EGFR) gene (3). Since mutations in EGFR constitutively act as an active receptor tyrosine kinase in NSCLC cells, several tyrosine kinase inhibitors, including gefitinib, have been developed and used as chemotherapeutic drugs to treat patients with NSCLC (4). Despite the initial clinical success of tyrosine kinase inhibitors (TKIs), acquired resistance to TKIs has developed in numerous patients with NSCLC (5). Much of the acquired resistance to TKIs has been associated with a secondary T790M mutation in EGFR (6,7). To overcome resistance to TKIs, several combined NSCLC treatments, such as erlotinib and cetuximab (8), afatinib and cetuximab (9), yuanhuadine and gefitinib (10), and metformin and gefitinib (11) have been proposed and studied). However, these therapeutic approaches often result in renewed drug resistance by activating alternative survival pathways (12-14).

Hypoxia is a characteristic of solid tumors, including NSCLC, that directly stimulates the malignant properties of cancer (15). In this tumor microenvironment, hypoxia-inducible factors (HIFs) are activated, and activated HIFs induce the expression of multiple genes associated with angiogenesis, metabolic regulation, cell apoptosis and tumor survival (16). The essential roles of HIFs in blood vessel formation and the recovery of the tumor blood supply make tumors difficult to treat, leading to resistance to radiotherapy, chemotherapy and immunotherapy (17). HIFs are heterodimeric transcription factors consisting of a HIF-α (HIF-α) and a constitutive β (HIF-β) subunits (18). The HIF-1α protein is strictly regulated by oxygen concentration in the tumor microenvironment (19). Due to hypoxia-specific expression and activity of HIF-1α in

tumorigenesis and escape from cancer therapy, HIF-1α may be a promising therapeutic target (20).

Gefitinib showed substantial efficacy in patients with NSCLC and active EGFR mutations (21). However, almost all patients who experience a marked response to gefitinib eventually develop progressive disease (21). This type of resistance has been observed in clinical trials, and includes primary and acquired resistance (22). Primary resistance usually occurs in patients with wild-type EGFR and other gene mutations downstream of the EGFR signaling pathway, such as the KRAS mutation (23). The acquired mutation is mainly due to the mutation T790M in the tyrosine kinase functional domain of EGFR (21). The T790M mutation is located in the ATP-/drug-binding cleft and triggers resistance by blocking the binding of gefitinib and the kinase domain (21).

In the present study, gefitinib was selected as the representative EGFR-TKI, and the differences between normal NSCLC and gefitinib-resistant (GR) NSCLC cell lines were investigated, focusing on HIF-1α protein expression and hypoxia-induced angiogenesis. The results showed that HIF-1α protein expression level and hypoxia-induced angiogenesis were increased in GR NSCLC cell lines. These results suggested that HIF-1α directly or indirectly regulated gefitinib resistance in NSCLC cell lines and could be a novel therapeutic target for combination treatment with EGFR-TKIs.

Materials and methods

Materials. Gefitinib was purchased from Sigma Aldrich; Merck KGaA. The HIF-1α antibodies were purchased from BD Pharmingen (BD Biosciences) and NOVUS Biologicals LLC.. The CD31 antibody was obtained from BD Pharmingen (BD Biosciences). The antibody against α-tubulin, MTT and cobalt chloride ($CoCl_2$) were all purchased from Sigma Aldrich; Merck KGaA. Matrigel was purchased from BD Pharmingen; BD Biosciences.

Cell culture, hypoxia treatment and transfection. The human NSCLC PC9 and HCC827 cell lines were purchased from Asan Medical Center and the American Type Culture Collection, respectively. The PC9/GR and HCC827/GR cell lines were generated as previously described (24,25). All the NSCLC cell lines were maintained in RPMI-1640 medium (Welgene, Inc.) supplemented with 10% FBS (HyClone; Cytiva) and 1% penicillin/streptomycin (Corning Life Sciences). The human dermal microvascular endothelial cell line (HMEC-1) was kindly provided by Dr Fransisco Candal Center for Disease Control and Prevention and maintained in MCDB131 medium (Gibco; Thermo Fisher Scientific, Inc.) supplemented with 10% FBS (HyClone; Cytiva), 1% penicillin/streptomycin, 10 mM L-glutamate (Gibco; Thermo Fisher Scientific, Inc.), 10 ng/ml epidermal growth factor (Sigma Aldrich; Merck KGaA) and 1 μg/ml hydrocortisone in a 37˚C humidified incubator with 5% CO_2 or in a hypoxic chamber (1% O_2, 5% CO_2 and 94% N_2; InvivO2; The Baker Company). The cell lines were inspected for mycoplasma contamination using a light microscope.

The vectors, pGIPZ, pGIPZ-V2LHS-132152 and pGIPZ-V2LHS-236718 were purchased from Open Biosystems Inc., (Thermo Fisher Scientific Inc.) and the latter 2 were used for short hairpin (sh)RNA vectors against human HIF-1A. pcDNA-HIF-1α for the overexpression of human HIF-1α and the pcDNA3.1 vector were a kind gift from Professor Gregg L. Semenza (Department of Medicine, Johns Hopkins School of Medicine, Baltimore, MD, USA). The PC9 cell line, in a 60-mm culture dish were transfected with 5 μg pGIPZ, pGIPZ-V2LHS-132152, pGIPZ-V2LHS-236718, pcDNA3.1 or pcDNA- HIF-1α using 4 μg/ml polyethyleneimine (Sigma Aldrich; Merck KGaA) at 37˚C for 6 h. pGIPZ or pcDNA3.1 was transfected and used as the control or mock. The media were replaced with fresh complete media, 6 h after transfection. The cells were used for subsequent experimentation 24 h after transfection.

MTT assay. The PC9, PC9/GR, HCC827 and HCC827/GR cells ($1x10^4$ cells per well) were plated in a 24-well plated and incubated with 0.1 μM gefitinib for 48 or 72 h in a 37˚C humidified incubator with 5% CO_2. MTT (0.1 mg/ml) was added to each well and incubated at 37˚C for 2 h, then dimethyl sulfoxide was added. The absorbance was measured at 560 nm using an iMark microplate absorbance reader (Bio-Rad Laboratories). All the data are presented as the mean ± SEM from three wells and from 3 independent experiments.

Colony formation assay. A total of 50 PC9 cells were plated on 60-mm dishes and were treated with increasing concentrations of gefitinib (10-200 nM) for 2 weeks at 37˚C in a humidified incubator with 5% CO_2. Following the incubation, RPMI-1640 medium (Welgene, Inc.) with 200 nM gefitinib and 10% FBS (HyClone; Cytiva) was removed, the cells were rinsed with PBS, fixed in acetic acid:methanol (1:7, vol/vol) for 5 min, and stained with crystal violet staining solution for 10 min, both at room temperature (RT). The number of colonies was counted under a light microscope. The data are presented as the mean ± SEM from 3 independent experiments.

Western blot analysis. The PC9, PC9/GR, HCC827 and HCC827/GR cell lines were incubated in a hypoxic chamber (37˚C; 1% O_2, 5% CO_2 and 94% N_2; InvivO2; The Baker Company) for 2, 8, 24 and 48 h. The cells were harvested and lysed in lysis buffer (50 mM Tris, 150 mM NaCl and 1% NP-40) supplemented with a protease inhibitor cocktail and phosphatase inhibitors (1 mM sodium orthovanadate and 10 mM sodium fluoride). The BCA method was used to determine the concentrations of the cell extracts. The cell extracts (30 μg/lane) were separated using 9% SDS-PAGE, then transferred to PVDF membranes (EMD Millipore). The membrane was blocked with 5% skimmed milk in TBS containing 0.1% Tween-20 for 1 h at room temperature, then incubated overnight at 4˚C with the appropriate primary antibodies. Next, the membrane was incubated with a HRP-conjugated secondary antibody (1:10,000; cat. no. PI-2000; Vector Laboratories; Maravai Lifesciences) for 1 h at room temperature. The signal was developed using an ECL western detection reagent (Thermo Fisher Scientific, Inc.). The following primary antibodies were used: Anti-HIF-1α (1:3,000; cat. no. 610958) and anti-α-tubulin (1:10,000; cat. no. T5168).

Conditioned media preparations. For preparation of conditioned medium (CM), the medium from the PC9 and PC9/GR cells was changed with 1% FBS (HyClone;

Cytiva)-containing RPMI-1640 (Welgene, Inc.) and further incubated for 16 h in a hypoxic chamber (37˚C; 1% O_2, 5% CO_2 and 94% N_2; InvivO2; The Baker Company). The CM was collected and filtered through a 0.22-μm pore membrane (EMD Millipore).

Wound healing assay. The HMEC-1 cell line ($1x10^5$) were plated on 24-well plates, cultured, then the monolayer was wounded with a micropipette tip and images of the cells were captured at 0 h time point. The attached HMEC-1 cells were incubated with growth medium mixed with 1 mM thymidine and CM collected from hypoxia-stimulated PC9 or PC9/GR cells for 16 h. Then, the cells were rinsed with PBS, fixed in absolute methanol for 5 min, stained with Giemsa (Sigma-Aldrich; Merck KGaA) for 10 min, both at RT, then images of each wound were captured at the same location. The migrated cells that moved beyond the reference line were counted and the number of migrated cells was divided by the number of unmigrated cells. The data are presented as the mean ± SEM from 3 independent experiments. The average migrated HMEC-1 cells, treated with CM from normoxic PC9 cells, was set to 100%.

Tube formation assay. A total of 200 μl Matrigel was polymerized on 24-well plates at 37˚C for 30 min. The HMEC-1 cell line ($1x10^5$) was seeded on the polymerized Matrigel and incubated with CM from either the hypoxia-stimulated PC9 or PC9/GR cell lines. After 16 h, morphological changes were observed and the areas of the tube branches were measured using ImageJ software v1.52 (National Institutes of Health). The data are presented as the mean ± SEM from 3 independent experiments. The average areas of the tube branches treated with CM from normoxic PC9 cells was set to 100%.

Rat aortic ring sprouting assay. The rat experiments were approved by the Committee for Care and Use of Laboratory Animals at the Kyung Hee University (KHUASP-20-289). A 6-week-old male Sprague Dawley rat (150-180 g) was purchased from Daehan Biolink and anesthetized with 30 mg/kg Zoletil and 10 mg/kg Rompun (26,27) by intraperitoneal injection. The aorta was extracted and the peri-aortic fibroadipose tissue was carefully removed. The rings were sliced at a thickness of 1 mm and randomly divided into 4 groups (PC9+normoxia, PC9/GR+normoxia, PC9+hypoxia and PC9/GR+hypoxia; n=3). Each ring was placed on polymerized Matrigel in each well of a 24-well plate, then covered with an additional 50 μl Matrigel. CM from hypoxia-stimulated PC9 or PC9/GR cell lines were added to each well for 5 days. Average sprouting was measured with ImageJ software v1.52 (National Institutes of Health) after images of the plates were captured. The data are presented as the mean ± SEM from 3 independent experiments. The average sprouting with CM from normoxic PC9 cells was set to 100%.

Mouse xenograft tumor model. All the mouse experiments were approved by the Committee for Care and Use of Laboratory Animals at the Kyung Hee University [KHUASP(SE)-17-144]. A total of 24 6-week-old male BALB/c nude mice were purchased from Daehan Biolink. The mice were housed 2-4 per cage and maintained under a controlled temperature (23±0.5˚C), humidity (50±10%) and a 12:12 h light:dark cycle, and food, drinking water and litter were changed every 2 days. The 7-week-old male mice (20-22 g) were randomly divided into 2 groups (PC9 and PC9/GR; n=12), anesthetized with 30 mg/kg Zoletil and 10 mg/kg Rompun (28,29), by intraperitoneal injection, then injected at a dorsal flank site with the PC9 or PC9/GR cell lines ($5x10^6$ cells per mouse), suspended in Matrigel, to perform subcutaneous tumorigenesis analysis. Their body weights and tumor sizes were measured every day for 3 weeks with a vernier caliper (Mitutoyo Corporation) and a digital balance, respectively. The tumor volume was calculated using the following formula: Tumor volume (mm^3) = 0.5 (width x length x height). After 3 weeks, the mice were euthanized with sodium pentobarbital (100 mg/kg), by intraperitoneal injection and the death of the mice was verified 10 min later by loss of movement, breath, heartbeat, corneal reflex and muscular tension. Before tumor extraction, subcutaneous tissue attached to each tumor was examined and images were captured under a light microscope. Microvessels could be detected by the naked eye. Extracted tumors were frozen with optimal cutting temperature (OCT) compound (Sigma-Aldrich; Merck KgaA) at -20˚C for 2 h and stored at -80˚C until use.

Immunohistochemical and immunofluorescent staining. OCT compound-frozen tumor tissues were sliced at a thickness of 10-μm and placed on gelatin-coated glass slides. The sectioned tissues were fixed with 4% paraformaldehyde at RT for 15 min and incubated with methanol containing 3% hydrogen peroxide for 20 min. To increase tumor permeability, the tissues were incubated with 0.3% Triton X-100 in PBS at RT for 20 min. The tissues were blocked with blocking solution [0.1% BSA (Sigma-Aldrich; Merck KgaA), 0.3% Triton X-100 and 1.5% FBS (HyClone; Cytiva)] at RT for 1 h, then incubated with the appropriate antibodies overnight at 4˚C. The tissues were subsequently washed with PBS and incubated with biotinylated anti-rabbit (cat. no. BA-1000) and anti-rat (cat. no. BA-4000) IgG (H+L) antibodies (1:500; Vector Laboratories; Maravai LifeSciences) or fluorescent anti-rabbit (cat. no. A11008) and anti-rat (cat. no. A21471) IgG (H+L) antibodies (1:500; Invitrogen; Thermo Fisher Scientific, Inc.) labeled secondary antibodies.

For biotinylation, the tissues were incubated with an Elite ABC kit (Vector laboratories, Maravai LifeSciences), and immunodetected by incubation with 3'3 diaminobenzidine (Sigma-Aldrich; Merck KgaA) solution at RT for 5 min. For fluorescence detection, the nuclei were stained with Hoechst 33342 (1:10,000; cat. no. 62249; Thermo Fisher Scientific, Inc.) at RT for 15 min. The following primary antibodies were used: Anti-HIF-1α (1:300; cat. no. NB100-479) and anti-CD31 (1:200; cat. no. 550274). Three random fields of view in each section were calculated using ImageJ software (National Institutes of Health) and the relative protein expression level of each protein was quantified according to integrated optical intensity from 3 independent experiments.

Statistical analysis. All the experiments were performed 3 times independently and the data are presented as the mean and SEM using SPSS software (v25; IBM Corp). Differences between 2 groups were evaluated using an unpaired Student's

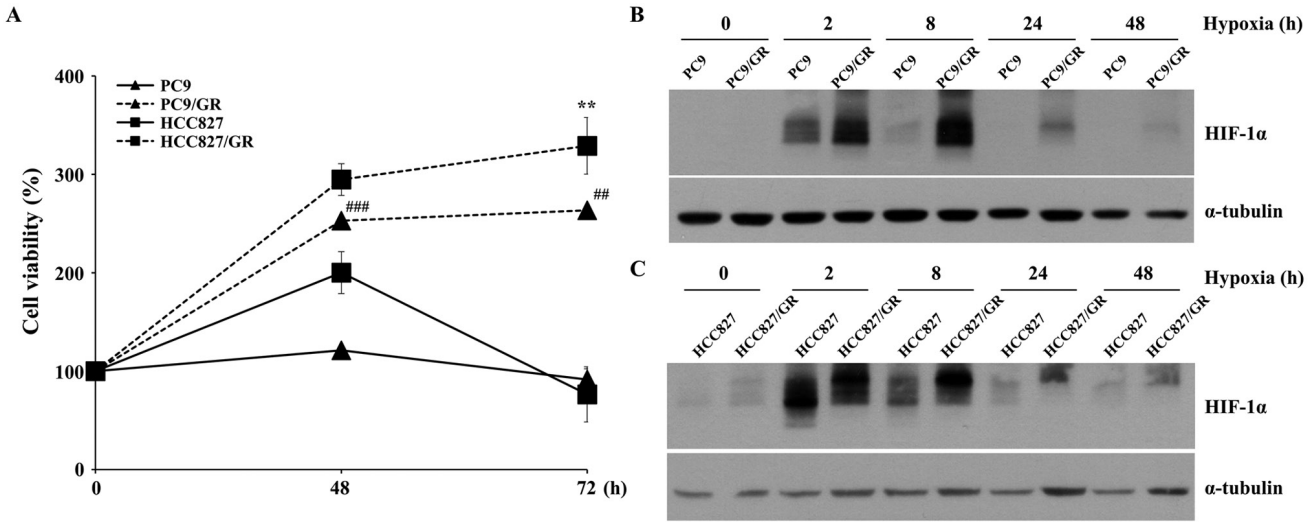

Figure 1. HIF-1α protein expression levels are increased in gefitinib-resistant non-small cell lung cancer cells lines (A) PC9, PC9/GR, HCC827 and HCC827/GR cell lines were treated with 0.1 μM gefitinib for 48 and 72 h. Cell viability was examined using a MTT assay and the data are presented as the mean ± SEM. (B) PC9, PC9/GR and (C) HCC827 and HCC827/GR cell lines were treated with gefitinib under hypoxic conditions for the indicated times, then the protein expression level of HIF-1α and α-tubulin was measured. **P<0.01 vs. PC9. $^{\#\#}$P<0.01 and $^{\#\#\#}$P<0.001 vs. HCC827.

t-test differences between 3 groups were evaluated by one-way ANOVA followed by a Tukey's post hoc test. P<0.05 was considered to indicate a statistically significant significance.

Results

HIF-1α protein expression levels were increased in GR NSCLC cell lines. To investigate the characteristics of GR NSCLC cell lines, PC9/GR and HCC827/GR were used in the present study. The GR cell lines were verified by analyzing the viabilities of these cells following treatment with gefitinib (Fig. 1A). Since HIF-1α is a key factor in tumor progression (30), HIF-1α protein expression levels in the PC9 and HCC827 cell lines were compared with that in the PC9/GR and HCC827/GR cell lines, respectively. As shown in Fig. 1B, the HIF-1α protein expression level in the PC9/GR cell line was higher compared with that in the PC9 cell line at all hypoxic exposure times tested. The same experimental results were observed between the HCC827 and HCC827/GR cell lines (Fig. 1C), indicating that hypoxia-induced HIF-1α protein expression levels were upregulated in GR NSCLC cell lines, and the PC9 cell line was selected for further analysis.

GR cell lines induce angiogenesis under hypoxic conditions. As HIF-1α mainly regulates hypoxia-induced angiogenesis during tumorigenesis (30,31), the angiogenic properties of GR NSCLC cell lines were analyzed using several angiogenesis assays and endothelial cells. The PC9 and PC9/GR cells were incubated under hypoxic conditions for 16 h, and CM was collected and administered to human microvascular endothelial cells, HMEC-1. As shown in Fig. 2A and B, the CM from hypoxia-stimulated PC9 cells induced the migration of the HMEC-1 cells. Furthermore, the induced migratory activity of the HMEC-1 cells was increased by CM from hypoxia-stimulated PC9/GR cells. To examine the tube-forming activities of the endothelial cells, a tube formation assay was performed using the HMEC-1 cells, treated with the aforementioned CM. Consistent with the migration assay, CM from hypoxia-stimulated PC9/GR cells increased hypoxia-induced tube formation (Fig. 2C and D). To confirm the increase in hypoxia-induced angiogenic activities in the HMEC-1 cells treated with PC9/GR CM, an *ex vivo* rat aortic ring sprouting assay was performed. As shown in Fig. 2E and F, the number of microvessels sprouting from the aortic ring was increased in the cells treated with CM from hypoxia-stimulated PC9/GR cells compared with that in cells treated with CM from hypoxia-stimulated PC9 cells. Furthermore, the hypoxic induction of angiogenic activities in the HMEC-1 treated with PC9/GR CM were higher compared with that in the HMEC-1 cells treated with PC9 CM (Fig. 2B, D and F). These results suggested that hypoxia-induced angiogenesis was increased by the PC9/GR cell line compared with that in the PC9 cell line, and that GR NSCLC cell lines could stimulate angiogenesis during tumorigenesis.

Tumor angiogenesis is increased in the GR cell lines. Tumor angiogenesis in GR tumors was subsequently investigated, as angiogenesis is an essential event in tumor progression (32). Tumor formation was induced by subcutaneously injecting PC9 and PC9/GR cells into BALB/c nude mice. As shown in Fig. 3A, the PC9 and PC9/GR tumors had a similar growth pattern and the body weight of the mice is shown in Fig. 3B. When the isolated tumors, 3 weeks after injection, were examined, there were no significant differences in tumor volume and weight between the PC9 and PC9/GR groups (Fig. 3C and D). The microvessels in the subcutaneous tissue attached to the tumors were also analyzed and the number of microvessels near the PC9/GR-derived tumors was increased compared with that near the PC9-derived tumors (Fig. 3E). To evaluate vessel formation within the tumors, it was examined whether the endothelial cells were present inside the tumors by staining for CD31, which is a specific marker of endothelial cells. As shown in Fig. 3F, the CD31 signal was increased in the PC9/GR tumors. Furthermore, it was found that the HIF-1α

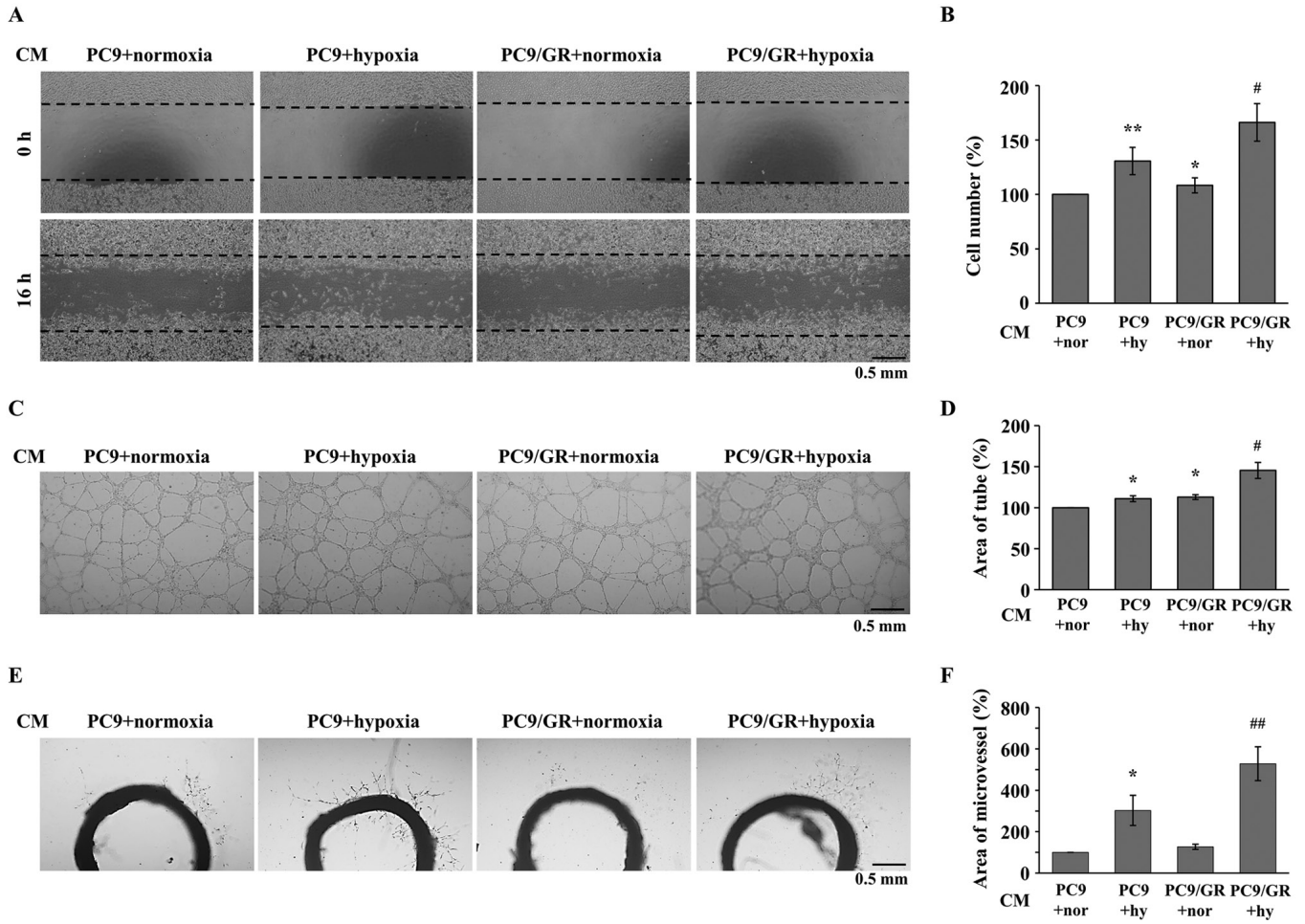

Figure 2. Gefitinib-resistant cells induced angiogenesis under hypoxic conditions. PC9 and PC9/GR cells were incubated under normoxic or hypoxic conditions for 24 h and CM was collected, and added to the HMEC-1 cells for further analysis (A) Wound healing assays were performed using HEMC-1 cells treated with CM from the PC9 and PC9/GR cells and (B) analyzed statistically. (C) Tube formation assays using the HMEC-1 cells were performed to determine the tube-forming abilities following treatment with CM from the PC9 and PC9/GR cells and the results were (D) quantified using ImageJ software and analyzed statistically. (E) Rat aortic ring sprouting assays were performed on aortic rings treated with CM from PC9 and PC9/GR cells and the results were (F) quantified and analyzed statistically. The data are presented as the mean ± SEM from 3 independent experiments. *P<0.05 and **P<0.01 vs. CM from PC9 cells under normoxic conditions; $^{\#}$P<0.05 and $^{\#\#}$P<0.01 vs. CM from hypoxia-stimulated PC9 cells. nor, normoxia; hy, hypoxia.

signal was also increased in the PC9/GR tumors (Fig. 3G). To confirm the association between HIF-1α expression and blood vessel formation, fluorescent double-staining was performed in the PC9 and PC9/GR tumors. In the PC9/GR tumor tissues, CD31 expression was increased around the HIF-1α-expressing region (Fig. 3H and I), indicating that HIF-1α-induced angiogenesis was stimulated in GR tumors.

Inhibiting HIF-1α attenuates the acquisition of GR in the NSCLC cell lines. To demonstrate the association between HIF-1α expression and gefitinib resistance, HIF-1α-regulated PC9 cells treated with $CoCl_2$, and transfected with shHIF-1A vector or HIF-1α overexpression vector were treated with increasing concentrations of gefitinib (from 10 to 200 nM) for 2 weeks in the colony formation assay. The PC9 cells were treated with $CoCl_2$ to induce the upregulation of HIF-1α expression (Fig. 4A) and a colony formation assay was performed following $CoCl_2$ and gefitinib treatment. As shown in Fig. 4B and C, $CoCl_2$ increased the number of PC9 colonies following gefitinib treatment. Next, shRNA vectors against HIF-1A were transfected into the PC9 cells (Fig. 4D) and were subsequently treated with $CoCl_2$ following which a colony formation assay was performed under $CoCl_2$ and gefitinib treatment. As shown in Fig. 4E and F, the colony forming activity was significantly inhibited by HIF-1α knockdown. On the contrary, HIF-1α overexpression vector was transfected into the PC9 cells (Fig. 4G) and a colony formation assay was performed under gefitinib treatment. As shown in Fig. 4H and I, number of colonies was significantly increased by HIF-1α overexpression, suggesting that HIF-1α induced gefitinib resistance in NSCLC cell lines.

Discussion

Chemotherapy using EGFR-TKIs has successfully improved the survival time in patients NSCLC; however, there are limitations to the use of EGFR-TKIs due to the acquisition of resistance (33). Gefitinib is a first-line treatment that has been used for patients with NSCLC, and acquired resistance inevitably develops (34). GR NSCLC promoted cell proliferation and exhibited more aggressive clinical progression (35). HIF-1 is a primary transcription factor that is activated by hypoxia, and induces the expression of various genes associated with

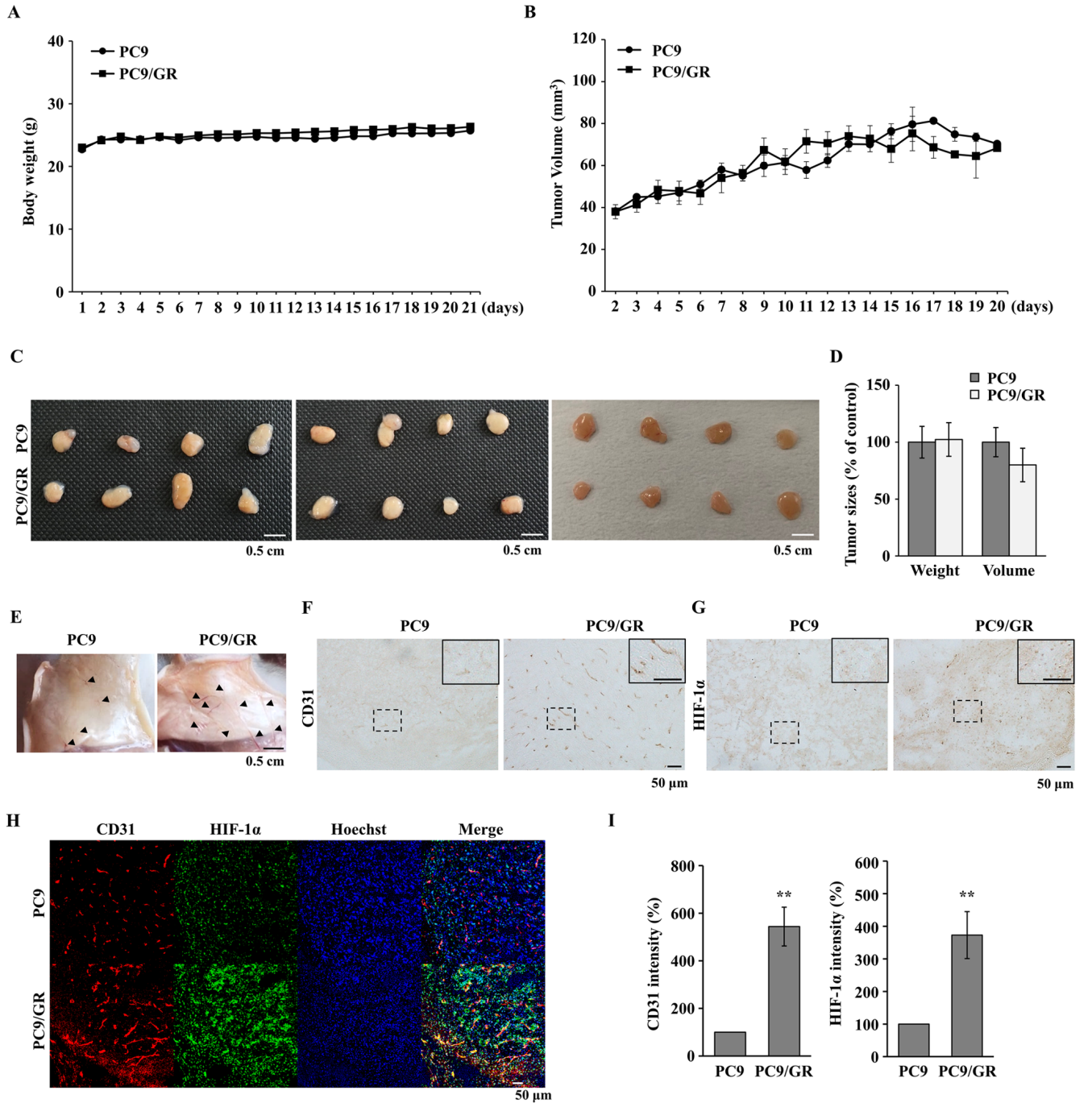

Figure 3. PC9 and PC9/GR tumors were generated in BALB/c nude mice and tumor angiogenesis was increased in PC9/GR tumors. BALB/c nude mice were injected with PC9 cells or PC9/GR cells, then (A) mouse weight and (B) tumor volume were measured using a digital balance and vernier caliper, respectively, every day for 3 weeks. (C) The mice were sacrificed, 3 weeks after the injection of the PC9 or PC9/GR cells and the tumors were isolated and images were captured, and (D) tumor volume and weight were measured. The data are presented as the mean ± SEM of 3 independent experiments with 4 mice per group (total 12 mice per group). (E) Blood vessels under the skin adjacent to the tumor tissues were examined. Arrowheads indicate visible blood vessels. Tumor sections were immunostained with specific antibodies for (F) CD31 and (G) HIF-1α. The squares with full black lines are the 2-fold magnified images for the dotted squares. (H) Double immunofluorescence staining was performed using specific antibodies against HIF-1α and CD31. Nuclei were stained with Hoechst 33342. (I) Signals for HIF-1α and CD31 were quantified using ImageJ software. The data are presented as the mean ± SEM from 3 independent experiments. $^{**}P<0.01$ vs. PC9 tumors.

angiogenesis, proliferation and survival during tumor progression (36). In addition, the accumulation of HIF-1α correlated with radiotherapy resistance and drug resistance to various cytotoxic agents (37-42). In the present study, it was found that GR tumors had increased HIF-1α protein expression level and tumor angiogenesis in NSCLC. This suggested that inhibition of HIF-1α may inhibit angiogenesis in GR NSCLC. Furthermore, in the PC9 cells treated with gefitinib, the regulation of HIF-1α controlled the acquisition of resistance. These findings indicate that HIF-1α could also be a potential target for overcoming acquired gefitinib resistance in NSCLC.

Due to signaling complexities and an increasing trend in anticancer drug resistance, a molecular target that plays a central role in diverse oncogenic signaling pathways has

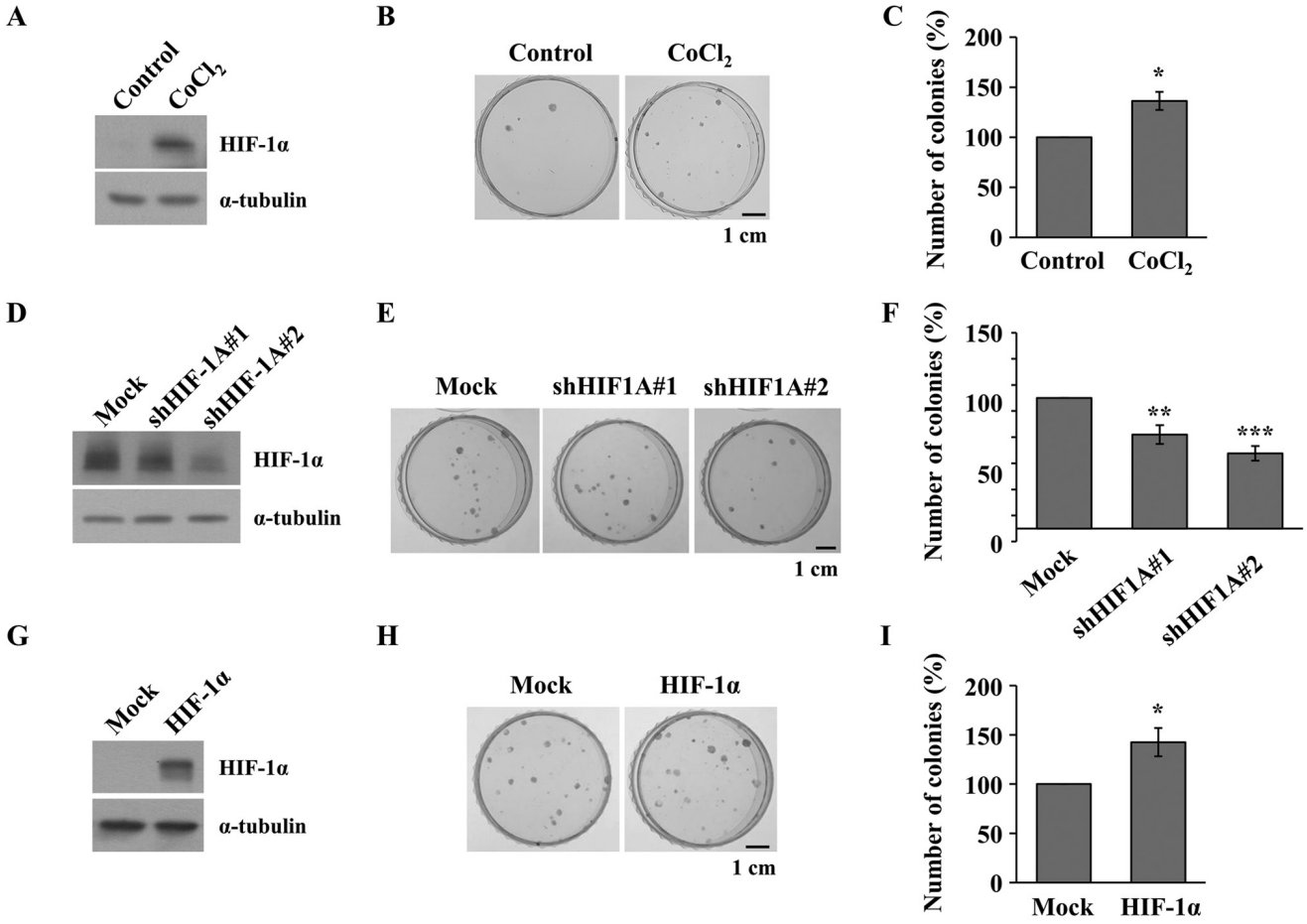

Figure 4. Inhibiting HIF-1α attenuates the acquisition of gefitinib resistance in the PC9 cell line. (A) PC9 cells were treated with $CoCl_2$ (20 μM) for 24 h and HIF-1α protein expression level was detected using western blot analysis. (B) Colony formation assay was performed to evaluate cell proliferation in the PC9 cells treated with $CoCl_2$ (20 μM) and increasing concentrations of gefitinib (from 10 to 200 nM). After 2 weeks, the colonies were stained, images were captured and (C) the colony numbers were analyzed from 3 independent experiments. *P<0.05 vs. control. (D) Western blot analysis was used to detect HIF-1α protein expression level in the PC9 cells transfected with shHIF-1A vectors. (E) Colony formation assay was performed in the shHIF-1A vectors-transfected PC9 cells treated with $CoCl_2$ (20 μM) and increasing concentrations of gefitinib (from 10 to 200 nM) and (F) the colony numbers were analyzed from 3 independent experiments. **P<0.01 and ***P<0.001 vs. Mock. pGIPZ was used as the mock. (G) HIF-1α protein expression level was determined using western blot analysis following transfection with HIF-1α overexpression vector. (H) Colony formation assay was performed in pcDNA-HIF-1α-transfected PC9 cells treated with increasing concentrations of gefitinib (from 10 to 200 nM) and (I) the colony numbers were analyzed from 3 independent experiments. The data are presented as the mean ± SEM. *P<0.05 vs. Mock. pcDNA3.1 was used as the mock. HIF-1α, pcDNA-HIF-1α; sh, short hairpin; shHIF-1A#1, pGIPZ-V2LHS-132152; shHIF-1A#2, pGIPZ-V2LHS-236718.

been investigated (43). A promising anticancer drug target, is HIF-1, which promotes physiological changes associated with therapeutic resistance, including the limitation of drug accumulation within cells and the regulation of the cellular response to chemotherapeutic agents (44-46). Previous studies have demonstrated that activation of HIF-1α inhibited doxorubicin-mediated apoptosis in human osteosarcoma (47), was associated with cisplatin resistance through the regulation of the glutamate-cysteine ligase modifier subunit and multidrug resistance (MDR)-associated proteins in lung cancer (48), and mediated resistance to cetuximab by the induction of glycolysis in head and neck squamous cell carcinoma cells (49,50). Numerous studies have suggested that HIF-1α was associated with the induction of the MDR1 gene, which encodes for and results in the overexpression of phospho-glycoprotein, a predominant membrane transporter associated with chemotherapy resistance (51). HIF-1α also induced the expression of pyruvate dehydrogenase kinase (PDK)-1 and -3, and the upregulation of PDK3 was associated with drug resistance in colon cancer (52). However, the mechanism by which HIF-1α mediates drug resistance in cancer is not fully understood. It was previously reported that HIF-1α expression was decreased in NSCLC cell lines following gefitinib treatment (53,54), and activation of HIF-1α in the HCC827 cell line stimulated tumorigenic activities, including proliferation and migration, even though gefitinib was administered for ~48 h (54). YC-1 enhanced the antitumor activity of gefitinib and reversed sensitivity to gefitinib in GR HCC827 cell lines (55,56). In the present study, the characteristics of GR NSCLC cell lines were analyzed and it was found that HIF-1α expression and angiogenic activities were increased in GR NSCLC cell lines and GR tumors compared with that in the parent NSCLC cell lines. Furthermore, overexpression of HIF-1α increased the number of colonies formed by gradually increasing concentrations of gefitinib-treated PC9 cells for 2 weeks; in contrast, knockdown of HIF-1α expression by shRNA vectors decreased the colony number. From the results, we hypothesized that regulation of HIF-1α may modulate the acquisition of gefitinib resistance in

NSCLC cell lines. In further studies, the related mechanism by which HIF-1α regulates the acquisition of gefitinib resistance should be examined.

Several studies support an association between EGFR activation and HIF-1α expression, which could be important in tumor progression (57-60). The EGF and EGFR signaling pathways might induce the translation of HIF-1α (57) and HIF-1α mediated angiogenesis by upregulating angiogenic factors, such as VEGF in tumor cells (61). In accordance with previous studies, the results in the present study indicated the induction of hypoxia-mediated tumor angiogenesis in GR NSCLC cell lines (Fig. 2). Previous studies have demonstrated that gefitinib reduced HIF-1α and VEGF protein expression levels in EGFR-sensitive NSCLC cell lines (57,62). HIF-1α expression is reduced by gefitinib; however, HIF-1α enhanced gefitinib resistance (54). We propose a possible mechanism to explain how downregulated HIF-1α controls gefitinib resistance. First, PI3K-AKT-FRAP signaling increases the rate of HIF-1α synthesis by other receptor and non-receptor tyrosine kinases, including HER2 and VSRC (63). Second, HIF-1α may increase c-Jun protein expression level, and a positive feed-forward loop exists between HIF-1α and c-Jun, in which constitutive activation of the JNK-c-Jun pathway can upregulate HIF-1α protein levels (64). Third, recent studies have revealed that HIF-1α was a direct transcriptional regulator of EGFR (59). EGFR enhances HIF-1α expression via a positive feed-forward loop (59). The induction of HIF-1α promotes EGFR transcription, and ultimately (59), EGFR mutations may be generated during the EGFR transcriptional process.

In conclusion, the results from the present study demonstrated that HIF-1α was increased in GR NSCLC cell lines and lead to induction of angiogenic effects in a mouse xenograft model and in angiogenesis assays *in vitro*. In addition, the regulation of HIF-1α controlled the proliferative ability of the PC9 cells under gefitinib treatment for two weeks. Therefore, HIF-1α could be a potential target for overcoming acquired gefitinib resistance using other EGFR-TKIs.

Acknowledgements

Not applicable.

Funding

This study was supported by the National Research Foundation of Korea grant funded by the Korea government (NRF-2021R1A2C1003297) and by a grant from the Basic Research Program through the National Research Foundation funded by the Ministry of Science and ICT (2019R1F1A1041812) of Republic of Korea.

Availability of data and materials

The datasets used and/or analyzed during the current study are available from the corresponding author on reasonable request.

Authors' contributions

SHL and JWJ designed the experiments. JEC, WYB and JSC performed the experiments and analyzed the data. WYB and JWJ wrote the paper. JEC, WYB, JSC, and JWJ confirm the authenticity of the data in the present manuscript. All authors read and approved the final version of the manuscript.

Ethics approval and consent to participate

All animal experiments were approved by the Committee for Care and Use of Laboratory Animals at the Kyung Hee University [KHUASP(SE)-17-144, 11-24-2017].

Patient consent for publication

Not applicable.

Competing interests

The authors declare that they have no competing interests.

References

1. Siegel RL, Miller KD and Jemal A: Cancer statistics, 2020. CA Cancer J Clin 70: 7-30, 2020.
2. Bray F, Ferlay J, Soerjomataram I, Siegel RL, Torre LA and Jemal A: Global cancer statistics 2018: GLOBOCAN estimates of incidence and mortality worldwide for 36 cancers in 185 countries. CA Cancer J Clin 68: 394-424, 2018.
3. Jackson AL, Zhou B and Kim WY: HIF, hypoxia and the role of angiogenesis in non-small cell lung cancer. Expert Opin Ther Targets 14: 1047-1057, 2010.
4. Nan X, Xie C, Yu X and Liu J: EGFR TKI as first-line treatment for patients with advanced EGFR mutation-positive non-small-cell lung cancer. Oncotarget 8: 75712-75726, 2017.
5. Dong L, Lei D and Zhang H: Clinical strategies for acquired epidermal growth factor receptor tyrosine kinase inhibitor resistance in non-small-cell lung cancer patients. Oncotarget 8: 64600-64606, 2017.
6. Nguyen KS, Kobayashi S and Costa DB: Acquired resistance to epidermal growth factor receptor tyrosine kinase inhibitors in non-small-cell lung cancers dependent on the epidermal growth factor receptor pathway. Clin Lung Cancer 10: 281-289, 2009.
7. Ma C, Wei S and Song Y: T790M and acquired resistance of EGFR TKI: A literature review of clinical reports. J Thorac Dis 3: 10-18, 2011.
8. Regales L, Gong Y, Shen R, de Stanchina E, Vivanco I, Goel A, Koutcher JA, Spassova M, Ouerfelli O, Mellinghoff IK, *et al*: Dual targeting of EGFR can overcome a major drug resistance mutation in mouse models of EGFR mutant lung cancer. J Clin Invest 119: 3000-3010, 2009.
9. Janjigian YY, Smit EF, Groen HJ, Horn L, Gettinger S, Camidge DR, Riely GJ, Wang B, Fu Y, Chand VK, *et al*: Dual inhibition of EGFR with afatinib and cetuximab in kinase inhibitor-resistant EGFR-mutant lung cancer with and without T790M mutations. Cancer Discov 4: 1036-1045, 2014.
10. Kim D, Bach DH, Fan YH, Luu TT, Hong JY, Park HJ and Lee SK: AXL degradation in combination with EGFR-TKI can delay and overcome acquired resistance in human non-small cell lung cancer cells. Cell Death Dis 10: 361, 2019.
11. Pan YH, Jiao L, Lin CY, Lu CH, Li L, Chen HY, Wang YB and He Y: Combined treatment with metformin and gefitinib overcomes primary resistance to EGFR-TKIs with EGFR mutation via targeting IGF-1R signaling pathway. Biologics 12: 75-86, 2018.
12. Zhuang H, Bai J, Chang JY, Yuan Z and Wang P: MTOR inhibition reversed drug resistance after combination radiation with erlotinib in lung adenocarcinoma. Oncotarget 7: 84688-84694, 2016.
13. Mok TSK, Kim SW, Wu YL, Nakagawa K, Yang JJ, Ahn MJ, Wang J, Yang JC, Lu Y, Atagi S, *et al*: Gefitinib Plus chemotherapy versus chemotherapy in epidermal growth factor receptor mutation-positive non-small-cell lung cancer resistant to first-line gefitinib (IMPRESS): Overall survival and biomarker analyses. J Clin Oncol 35: 4027-4034, 2017.

14. Zhuang H, Shi S, Guo Y and Wang Z: Increase of secondary mutations may be a drug-resistance mechanism for lung adenocarcinoma after radiation therapy combined with tyrosine kinase inhibitor. J Cancer 10: 5371-5376, 2019.
15. Muz B, de la Puente P, Azab F and Azab AK: The role of hypoxia in cancer progression, angiogenesis, metastasis, and resistance to therapy. Hypoxia (Auckl) 3: 83-92, 2015.
16. Majmundar AJ, Wong WJ and Simon MC: Hypoxia-inducible factors and the response to hypoxic stress. Mol Cell 40: 294-309, 2010.
17. Tatum JL, Kelloff GJ, Gillies RJ, Arbeit JM, Brown JM, Chao KS, Chapman JD, Eckelman WC, Fyles AW, Giaccia AJ, *et al*: Hypoxia: Importance in tumor biology, noninvasive measurement by imaging, and value of its measurement in the management of cancer therapy. Int J Radiat Biol 82: 699-757, 2006.
18. Ziello JE, Jovin IS and Huang Y: Hypoxia-inducible factor (HIF)-1 regulatory pathway and its potential for therapeutic intervention in malignancy and ischemia. Yale J Biol Med 80: 51-60, 2007.
19. Jing X, Yang F, Shao C, Wei K, Xie M, Shen H and Shu Y: Role of hypoxia in cancer therapy by regulating the tumor microenvironment. Mol Cancer 18: 157, 2019.
20. Jin X, Dai L, Ma Y, Wang J and Liu Z: Implications of HIF-1α in the tumorigenesis and progression of pancreatic cancer. Cancer Cell Int 20: 273, 2020.
21. Li H, Zhou S, Li X, Wang D, Wang Y, Zhou C and Schmid-Bindert G: Gefitinib-resistance is related to BIM expression in non-small cell lung cancer cell lines. Cancer Biother Radiopharm 28: 115-123, 2013.
22. Sharma P, Hu-Lieskovan S, Wargo JA and Ribas A: Primary, adaptive, and acquired resistance to cancer immunotherapy. Cell 168: 707-723, 2017.
23. Pao W, Miller VA, Politi KA, Riely GJ, Somwar R, Zakowski MF, Kris MG and Varmus H: Acquired resistance of lung adenocarcinomas to gefitinib or erlotinib is associated with a second mutation in the EGFR kinase domain. PLoS Med 2: e73, 2005.
24. He J, Jin S, Zhang W, Wu D, Li J, Xu J and Gao W: Long non-coding RNA LOC554202 promotes acquired gefitinib resistance in non-small cell lung cancer through upregulating miR-31 expression. J Cancer 10: 6003-6013, 2019.
25. Nigro A, Ricciardi L, Salvato I, Sabbatino F, Vitale M, Crescenzi MA, Montico B, Triggiani M, Pepe S, Stellato C, *et al*: Enhanced expression of CD47 is associated with off-target resistance to tyrosine kinase inhibitor gefitinib in NSCLC. Front Immunol 10: 3135, 2020.
26. Del Signore A, Gotti C, Rizzo A, Moretti M and Paggi P: Nicotinic acetylcholine receptor subtypes in the rat sympathetic ganglion: Pharmacological characterization, subcellular distribution and effect of pre- and postganglionic nerve crush. J Neuropathol Exp Neurol 63: 138-150, 2004.
27. Kim AR, Kim JH, Kim A, Sohn Y, Cha JH, Bak EJ and Yoo YJ: Simvastatin attenuates tibial bone loss in rats with type 1 diabetes and periodontitis. J Transl Med 16: 306, 2018.
28. Pacioni S, Rueger MA, Nisticò G, Bornstein SR, Park DM, McKay RD and Androutsellis-Theotokis A: Fast, potent pharmacological expansion of endogenous $hes3^{+}/sox2^{+}$ cells in the adult mouse and rat hippocampus. PLoS One 7: e51630, 2012.
29. Kwon TR, Han SW, Kim JH, Lee BC, Kim JM, Hong JY and Kim BJ: Polydeoxyribonucleotides improve diabetic wound healing in mouse animal model for experimental validation. Ann Dermatol 31: 403-413, 2019.
30. Maxwell PH, Dachs GU, Gleadle JM, Nicholls LG, Harris AL, Stratford IJ, Hankinson O, Pugh CW and Ratcliffe PJ: Hypoxia-inducible factor-1 modulates gene expression in solid tumors and influences both angiogenesis and tumor growth. Proc Natl Acad Sci USA 94: 8104-8109, 1997.
31. Carmeliet P, Dor Y, Herbert JM, Fukumura D, Brusselmans K, Dewerchin M, Neeman M, Bono F, Abramovitch R, Maxwell P, *et al*: Role of HIF-1alpha in hypoxia-mediated apoptosis, cell proliferation and tumour angiogenesis. Nature 394: 485-490, 1998.
32. Folkman J: What is the evidence that tumors are angiogenesis dependent? J Natl Cancer Inst 82: 4-6, 1990.
33. Lin JJ and Shaw AT: Resisting resistance: Targeted therapies in lung cancer. Trends Cancer 2: 350-364, 2016.
34. Gao J, Li HR, Jin C, Jiang JH and Ding JY: Strategies to overcome acquired resistance to EGFR TKI in the treatment of non-small cell lung cancer. Clin Transl Oncol 21: 1287-1301, 2019.
35. Qi M, Tian Y, Li W, Li D, Zhao T, Yang Y, Li Q, Chen S, Yang Y, Zhang Z, *et al*: ERK inhibition represses gefitinib resistance in non-small cell lung cancer cells. Oncotarget 9: 12020-12034, 2018.
36. Semenza GL: HIF-1 and human disease: One highly involved factor. Genes Dev 14: 1983-1991, 2000.
37. Chen L, Feng P, Li S, Long D, Cheng J, Lu Y and Zhou D: Effect of hypoxia-inducible factor-1alpha silencing on the sensitivity of human brain glioma cells to doxorubicin and etoposide. Neurochem Res 34: 984-990, 2009.
38. Nardinocchi L, Puca R, Sacchi A and D'Orazi G: Inhibition of HIF-1alpha activity by homeodomain-interacting protein kinase-2 correlates with sensitization of chemoresistant cells to undergo apoptosis. Mol Cancer 8: 1, 2009.
39. Hao J, Song X, Song B, Liu Y, Wei L, Wang X and Yu J: Effects of lentivirus-mediated HIF-1alpha knockdown on hypoxia-related cisplatin resistance and their dependence on p53 status in fibrosarcoma cells. Cancer Gene Ther 15: 449-455, 2008.
40. Liu L, Ning X, Sun L, Zhang H, Shi Y, Guo C, Han S, Liu J, Sun S, Han Z, *et al*: Hypoxia-inducible factor-1 alpha contributes to hypoxia-induced chemoresistance in gastric cancer. Cancer Sci 99: 121-128, 2008.
41. Sasabe E, Zhou X, Li D, Oku N, Yamamoto T and Osaki T: The involvement of hypoxia-inducible factor-1alpha in the susceptibility to gamma-rays and chemotherapeutic drugs of oral squamous cell carcinoma cells. Int J Cancer 120: 268-277, 2007.
42. Brown LM, Cowen RL, Debray C, Eustace A, Erler JT, Sheppard FC, Parker CA, Stratford IJ and Williams KJ: Reversing hypoxic cell chemoresistance in vitro using genetic and small molecule approaches targeting hypoxia inducible factor-1. Mol Pharmacol 69: 411-418, 2006.
43. von Manstein V, Yang CM, Richter D, Delis N, Vafaizadeh V and Groner B: Resistance of cancer cells to targeted therapies through the activation of compensating signaling loops. Curr Signal Transduct Ther 8: 193-202, 2013.
44. Unruh A, Ressel A, Mohamed HG, Johnson RS, Nadrowitz R, Richter E, Katschinski DM and Wenger RH: The hypoxia-inducible factor-1 alpha is a negative factor for tumor therapy. Oncogene 22: 3213-3220, 2003.
45. Verduzco D, Lloyd M, Xu L, Ibrahim-Hashim A, Balagurunathan Y, Gatenby RA and Gillies RJ: Intermittent hypoxia selects for genotypes and phenotypes that increase survival, invasion, and therapy resistance. PLoS One 10: e0120958, 2015.
46. Zhao Q, Li Y, Tan BB, Fan LQ, Yang PG and Tian Y: HIF-1α induces multidrug resistance in gastric cancer cells by inducing miR-27a. PLoS One 10: e0132746, 2015.
47. Roncuzzi L, Pancotti F and Baldini N: Involvement of HIF-1α activation in the doxorubicin resistance of human osteosarcoma cells. Oncol Rep 32: 389-394, 2014.
48. Li F, Zhu T, Cao B, Wang J and Liang L: Apatinib enhances antitumour activity of EGFR-TKIs in non-small cell lung cancer with EGFR-TKI resistance. Eur J Cancer 84: 184-192, 2017.
49. Lu H, Lu Y, Xie Y, Qiu S, Li X and Fan Z: Rational combination with PDK1 inhibition overcomes cetuximab resistance in head and neck squamous cell carcinoma. JCI Insight 4: 4, 2019.
50. Lu H, Liang K, Lu Y and Fan Z: The anti-EGFR antibody cetuximab sensitizes human head and neck squamous cell carcinoma cells to radiation in part through inhibiting radiation-induced upregulation of HIF-1α. Cancer Lett 322: 78-85, 2012.
51. Comerford KM, Wallace TJ, Karhausen J, Louis NA, Montalto MC and Colgan SP: Hypoxia-inducible factor-1-dependent regulation of the multidrug resistance (MDR1) gene. Cancer Res 62: 3387-3394, 2002.
52. Lu CW, Lin SC, Chien CW, Lin SC, Lee CT, Lin BW, Lee JC and Tsai SJ: Overexpression of pyruvate dehydrogenase kinase 3 increases drug resistance and early recurrence in colon cancer. Am J Pathol 179: 1405-1414, 2011.
53. Rho JK, Choi YJ, Lee JK, Ryoo BY, Na II, Yang SH, Kim CH, Yoo YD and Lee JC: Gefitinib circumvents hypoxia-induced drug resistance by the modulation of HIF-1alpha. Oncol Rep 21: 801-807, 2009.
54. Jin Q, Zhou J, Xu X, Huang F and Xu W: Hypoxia-inducible factor-1 signaling pathway influences the sensitivity of HCC827 cells to gefitinib. Oncol Lett 17: 4034-4043, 2019.
55. Hu H, Miao XK, Li JY, Zhang XW, Xu JJ, Zhang JY, Zhou TX, Hu MN, Yang WL and Mou LY: YC-1 potentiates the antitumor activity of gefitinib by inhibiting HIF-1α and promoting the endocytic trafficking and degradation of EGFR in gefitinib-resistant non-small-cell lung cancer cells. Eur J Pharmacol 874: 172961, 2020.

56. Jin Q, Zheng J, Chen M, Jiang N, Xu X and Huang F: HIF-1 inhibitor YC-1 reverses the acquired resistance of EGFR-mutant HCC827 cell line with MET amplification to gefitinib. Oxid Med Cell Longev 2021: 6633867, 2021.
57. Pore N, Jiang Z, Gupta A, Cerniglia G, Kao GD and Maity A: EGFR tyrosine kinase inhibitors decrease VEGF expression by both hypoxia-inducible factor (HIF)-1-independent and HIF-1-dependent mechanisms. Cancer Res 66: 3197-3204, 2006.
58. Lee SH, Koo KH, Park JW, Kim HJ, Ye SK, Park JB, Park BK and Kim YN: HIF-1 is induced via EGFR activation and mediates resistance to anoikis-like cell death under lipid rafts/caveolae-disrupting stress. Carcinogenesis 30: 1997-2004, 2009.
59. Peng XH, Karna P, Cao Z, Jiang BH, Zhou M and Yang L: Cross-talk between epidermal growth factor receptor and hypoxia-inducible factor-1alpha signal pathways increases resistance to apoptosis by up-regulating survivin gene expression. J Biol Chem 281: 25903-25914, 2006.
60. Swinson DE and O'Byrne KJ: Interactions between hypoxia and epidermal growth factor receptor in non-small-cell lung cancer. Clin Lung Cancer 7: 250-256, 2006.
61. Tang N, Wang L, Esko J, Giordano FJ, Huang Y, Gerber HP, Ferrara N and Johnson RS: Loss of HIF-1alpha in endothelial cells disrupts a hypoxia-driven VEGF autocrine loop necessary for tumorigenesis. Cancer Cell 6: 485-495, 2004.
62. Lee JG and Wu R: Erlotinib-cisplatin combination inhibits growth and angiogenesis through c-MYC and HIF-1α in EGFR-mutated lung cancer in vitro and in vivo. Neoplasia 17: 190-200, 2015.
63. Laughner E, Taghavi P, Chiles K, Mahon PC and Semenza GL: HER2 (neu) signaling increases the rate of hypoxia-inducible factor 1alpha (HIF-1alpha) synthesis: Novel mechanism for HIF-1-mediated vascular endothelial growth factor expression. Mol Cell Biol 21: 3995-4004, 2001.
64. Meng S, Wang G, Lu Y and Fan Z: Functional cooperation between HIF-1α and c-Jun in mediating primary and acquired resistance to gefitinib in NSCLC cells with activating mutation of EGFR. Lung Cancer 121: 82-90, 2018.